Cancer Cell
Article

Angiopoietin-like 4 Protein Elevates the Prosurvival Intracellular O_2^-:H_2O_2 Ratio and Confers Anoikis Resistance to Tumors

Pengcheng Zhu,[1] Ming Jie Tan,[1] Royston-Luke Huang,[1] Chek Kun Tan,[1] Han Chung Chong,[1] Mintu Pal,[1] Chee Ren Ivan Lam,[1] Petra Boukamp,[2] Jiun Yit Pan,[3] Suat Hoon Tan,[3] Sander Kersten,[4] Hoi Yeung Li,[1] Jeak Ling Ding,[5] and Nguan Soon Tan[1,*]

[1]School of Biological Sciences, Nanyang Technological University, 60 Nanyang Drive, Singapore 637551, Singapore
[2]Division of Genetics of Skin Carcinogenesis, German Cancer Research Center (DKFZ), Im Neuenheimer Feld 280, D-69120 Heidelberg, Germany
[3]National Skin Centre, 1 Mandalay Road, Singapore 308205, Singapore
[4]Nutrition, Metabolism and Genomics Group, Wageningen University, 6700 EV Wageningen, The Netherlands
[5]Department of Biological Sciences, National University of Singapore, 14 Science Drive, Singapore 117543, Singapore
*Correspondence: nstan@ntu.edu.sg
DOI 10.1016/j.ccr.2011.01.018

SUMMARY

Cancer is a leading cause of death worldwide. Tumor cells exploit various signaling pathways to promote their growth and metastasis. To our knowledge, the role of angiopoietin-like 4 protein (ANGPTL4) in cancer remains undefined. Here, we found that elevated ANGPTL4 expression is widespread in tumors, and its suppression impairs tumor growth associated with enhanced apoptosis. Tumor-derived ANGPTL4 interacts with integrins to stimulate NADPH oxidase-dependent production of O_2^-. A high ratio of O_2^-:H_2O_2 oxidizes/activates Src, triggering the PI3K/PKBα and ERK prosurvival pathways to confer anoikis resistance, thus promoting tumor growth. ANGPTL4 deficiency results in diminished O_2^- production and a reduced O_2^-:H_2O_2 ratio, creating a cellular environment conducive to apoptosis. ANGPTL4 is an important redox player in cancer and a potential therapeutic target.

INTRODUCTION

In response to stresses such as hypoxia and inflammation in the tumor microenvironment, tumor cells exploit various signaling molecules to sustain and promote their growth, invasiveness, and metastasis (Singh et al., 2007). Aggressive tumor metastasis and invasiveness are the main cause of mortality in patients with cancer (Fidler, 1999). The constitutive activation of intracellular signaling by these molecules in tumor cells leads to cellular changes, including increased proliferation and the ability for cells to grow beyond their original confined milieu, leading to metastasis (Pani et al., 2009; Westhoff and Fulda, 2009). Among these changes, the loss of dependence on integrin-mediated extracellular matrix contact for growth (i.e., anoikis resistance) is an essential feature of tumor cells. However, the mechanism by which anoikis resistance is acquired remains an unsolved problem in cancer biology.

Although low levels of reactive oxygen species (ROS) regulate cellular signaling and play an important role in normal cell proliferation, recent studies show that tumors exhibit an excessive amount or persistent elevation of ROS (specifically the superoxide anion O_2^-) and utilize a redox-based mechanism to evade death by anoikis (Chiarugi, 2008; Giannoni et al., 2008; Pervaiz and Clément, 2007). Previous studies have indicated that ROS are involved in tumor initiation, progression, and maintenance. Furthermore, deregulated ROS production is also associated

Significance

We show here that elevated expression of ANGPTL4 is widespread in tumors, and tumor-derived ANGPTL4 confers anoikis resistance to tumors via autocrine adhesion mimicry. Our findings that ANGPTL4 hijacks integrin-mediated signaling to maintain an elevated, oncogenic O_2^-:H_2O_2 ratio and, therefore, confers anoikis resistance to tumor cells suggest ANGPTL4 as an important player in redox-mediated cancer progression. Treating cancer cells with ANGPTL4-targeted RNAi or monoclonal antibodies imparts a significant decrease in in vivo tumor growth and induces apoptosis in cancer cell lines upon anoikis challenge. Our findings suggest that anticancer strategies focusing on redox-based apoptosis induction in tumors are viable.

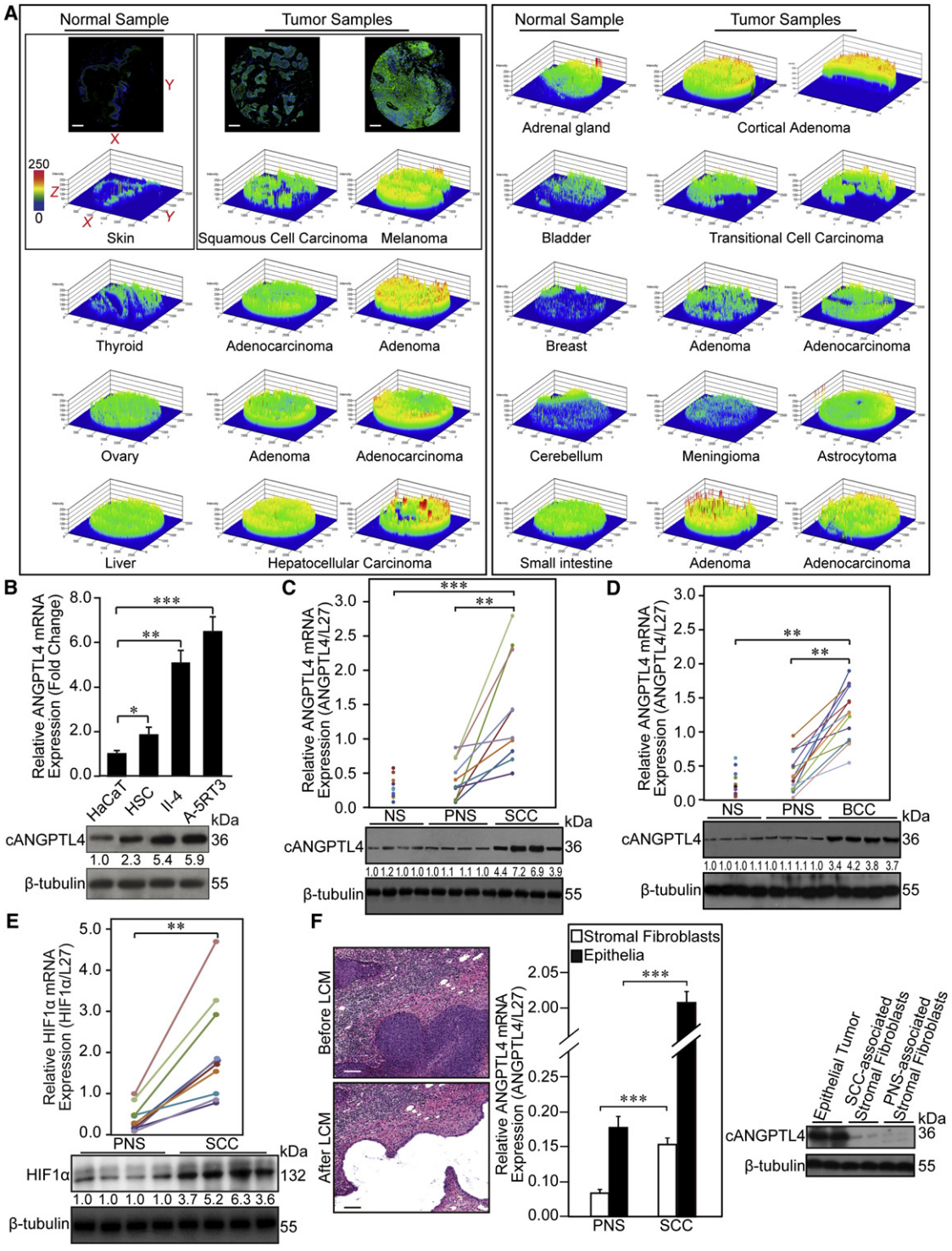

Figure 1. Elevated Expression of ANGPTL4 in Various Tumor Types

(A) ANGPTL4 expression varied among tumors procured from different anatomic sites. Heat map profiles generated from IF images. X, Y, and Z axes represent the length, width, and IF intensity, respectively. Representative images of normal skin and tumor samples with their corresponding heat maps are shown. Heat maps from same anatomic sites are grouped horizontally. Results are representative of two independent experiments performed in duplicate. Scale bars represent 200 μm.

(B) Relative ANGPTL4 mRNA and protein levels in nontumorigenic skin cell HaCaT and tumorigenic lines HSC, II-4, and A-5RT3.

(C and D) Relative ANGPTL4 mRNA and protein levels in paired human SCCs (C) or BCCs (D) and cognate PNSs. Normal human skin (NS) biopsies serve as additional controls. Three SSCs with the highest mRNA ANGPTL4 levels corresponded to an invasive prognosis.

with an invasive tumor phenotype. Oncogenic and mitogenic Ras activity is superoxide dependent, and a sustained increase in ROS following the overexpression of Nox1 (the catalytic subunit of NADPH oxidase) leads to cell transformation and aggressive tumor metastasis (Komatsu et al., 2008; Suh et al., 1999). Elevated production of ROS following activation of the c-Met proto-oncogene leads to cell transformation and malignant growth (Ferraro et al., 2006), and Rac-dependent redox signals increase the secretion of metalloproteinases and induce epithelial-mesenchymal transition (Wu, 2006), two key features of invasive cancers. Thus, a clear understanding of the underlying redox-based anoikis escape mechanism and its connection to malignancy will provide insight into therapeutic interventions.

The secreted protein angiopoietin-like 4 (ANGPTL4) was recently linked to tumor progression. ANGPTL4 was previously identified as a paracrine and, possibly, endocrine regulator of lipid metabolism (Oike et al., 2005) and a target of peroxisome proliferators-activated receptors (PPARs) (Kersten et al., 2000). ANGPTL4 is expressed in numerous cell types, such as adipocytes and hepatocytes, and is upregulated after fasting and hypoxia (Belanger et al., 2002; Kersten et al., 2000). Importantly, ANGPTL4 undergoes proteolytic processing to release its C-terminal fibrinogen-like domain (cANGPTL4), which circulates as a monomer but whose function remains unclear. The N-terminal coiled-coil domain of ANGPTL4 (nANGPTL4) mediates ANGPTL4 oligomerization and binds to lipoprotein lipase to modulate lipoprotein metabolism (Ge et al., 2004). Emerging studies also implicate tumor-derived ANGPTL4 in cancer metastasis via its effect on endothelial integrity. However, whether ANGPTL4 promotes or inhibits vascular permeability and, thus, cancer metastasis remains controversial. Several previous studies suggest that ANGPTL4 can prevent metastasis by inhibiting vascular leakiness (Galaup et al., 2006; Ito et al., 2003). Conversely, ANGPTL4 is also implicated as a pro-angiogenic factor (Le Jan et al., 2003). Recent reports demonstrate that *ANGPTL4* is one of the most highly predictive genes associated with breast cancer metastasis to the lung (Minn et al., 2005; Padua et al., 2008). ANGPTL4 expression is upregulated in clear cell renal-cell carcinoma (Le Jan et al., 2003) and oral tongue squamous cell carcinoma (SCC) (Wang et al., 2010). In addition, tumor-derived ANGPTL4 has been shown to promote metastasis by disrupting vascular integrity (Padua et al., 2008). The reasons for these conflicting results and the underlying mechanism of ANGPTL4 activity in tumor cells have not been clarified, hampering our understanding of its precise role in cancer metastasis. More importantly, the global expression pattern of ANGPTL4 in different types of tumors, to our knowledge, has yet to be fully investigated, and the pathological relevance of ANGPTL4 in cancer biology remains largely undefined. Thus, we set up to study the role of ANGPTL4 in tumor growth and metastasis.

RESULTS

Elevated Expression of ANGPTL4 in Various Tumor Types

To examine the expression profile of ANGPTL4 in human tumors, we screened its expression pattern on two human tumor tissue arrays, which cover most of the common benign, malignant, and metastatic tumors originating from various anatomic sites. Using immunofluorescence (IF) with an anti-cANGPTL4 antibody, we observed widespread, elevated ANGPTL4 expression in all epithelial tumor samples when compared to the corresponding normal tissues, regardless of the anatomic sites of origin (Figure 1A; see Figures S1A and S1B available online). However, the IF signal level varied among different types of tumors. Notably, the expression of ANGPTL4 increased as tumors progressed from a benign state to an invasive/metastatic state (Figure S1C). Next, we determined ANGPTL4 expression on three human skin tumorigenic lines (HSC, II-4, and A-5RT3), ten human SCC, and 13 basal cell carcinoma (BCC) biopsies by quantitative real-time PCR (qPCR) and immunoblot analyses. Consistent with our prior results, we observed increased ANGPTL4 mRNA and protein levels in these epithelial tumor cells compared with the nontumorigenic human skin line HaCaT or cognate peri-tumor normal samples (PNSs), respectively (Figures 1B–1D). No difference was observed between normal skin biopsies (NSs) and PNSs (Figures 1C and 1D). Interestingly, the three SCCs expressing the highest mRNA level of ANGPTL4 corresponded to an invasive prognosis (Figure 1C), underscoring our finding from tumor tissue arrays. In addition, polyclonal antibodies against either the N or C terminus of ANGPTL4 detected only cANGPTL4 in these tumor lines and SSCs (Figures 1B–1D; Figure S1D and S1E). To understand the reason for the increased expression of ANGPTL4 in tumor cells, we examined the expression of hypoxia-inducible factor 1 α (HIF1α) and PPARs in the SCCs. We found a concomitant upregulation of HIF1α with ANGPTL4 in SSCs than in PNSs (correlation coefficient = 0.88) (Figure 1E; Figures S1F). No clear correlation was observed between the expression of ANGPTL4 and the three PPAR isotypes (Figures S1G–S1I). These results suggested that at least for SCCs, the elevated ANGPTL4 expression reflects the tumor's hypoxic microenvironment. As a protein that is secreted by tumor cells, ANGPTL4 may perform paracrine or autocrine function in tumors. Therefore, we sought to determine the source of ANGPTL4 in tumors. We isolated epithelial tumor and stromal tissues, the latter consisting mainly of fibroblasts, from SCCs and PNSs, using laser capture microdissection (LCM). qPCR and immunoblot analyses revealed that epithelial tumor cells, rather than tumor stroma, were the major contributor of ANGPTL4 in SCCs (Figure 1F). Furthermore, only a low, baseline level of ANGPTL4 expression was found in normal PNS stroma and epithelia, suggesting that ANGPTL4 may have an autocrine role in tumors.

(E) Relative HIF1α mRNA and protein levels in paired SCCs and PNSs. For qPCR results, data points from the same individual are linked by colored lines.
(F) Relative ANGPTL4 mRNA and protein levels in LCM epithelial cells and stromal fibroblasts from paired SCCs and PNSs. Hematoxylin and eosin images of an SCC section before and after LCM of epithelial tissue are shown in left panel. Scale bars represent100 μm. Microdissected tissues were processed for qPCR (middle panel) and immunoblotting (right panel).
(B–F) mRNA data (mean ± SD) are from two independent qPCR experiments performed in triplicate. Ribosomal protein L27 (L27) serves as a reference housekeeping gene. *$p < 0.05$; **$p < 0.01$; ***$p < 0.001$. Immunoblot data are from three independent experiments performed in duplicate. β-Tubulin serves as a loading and transfer control. See also Figure S1.

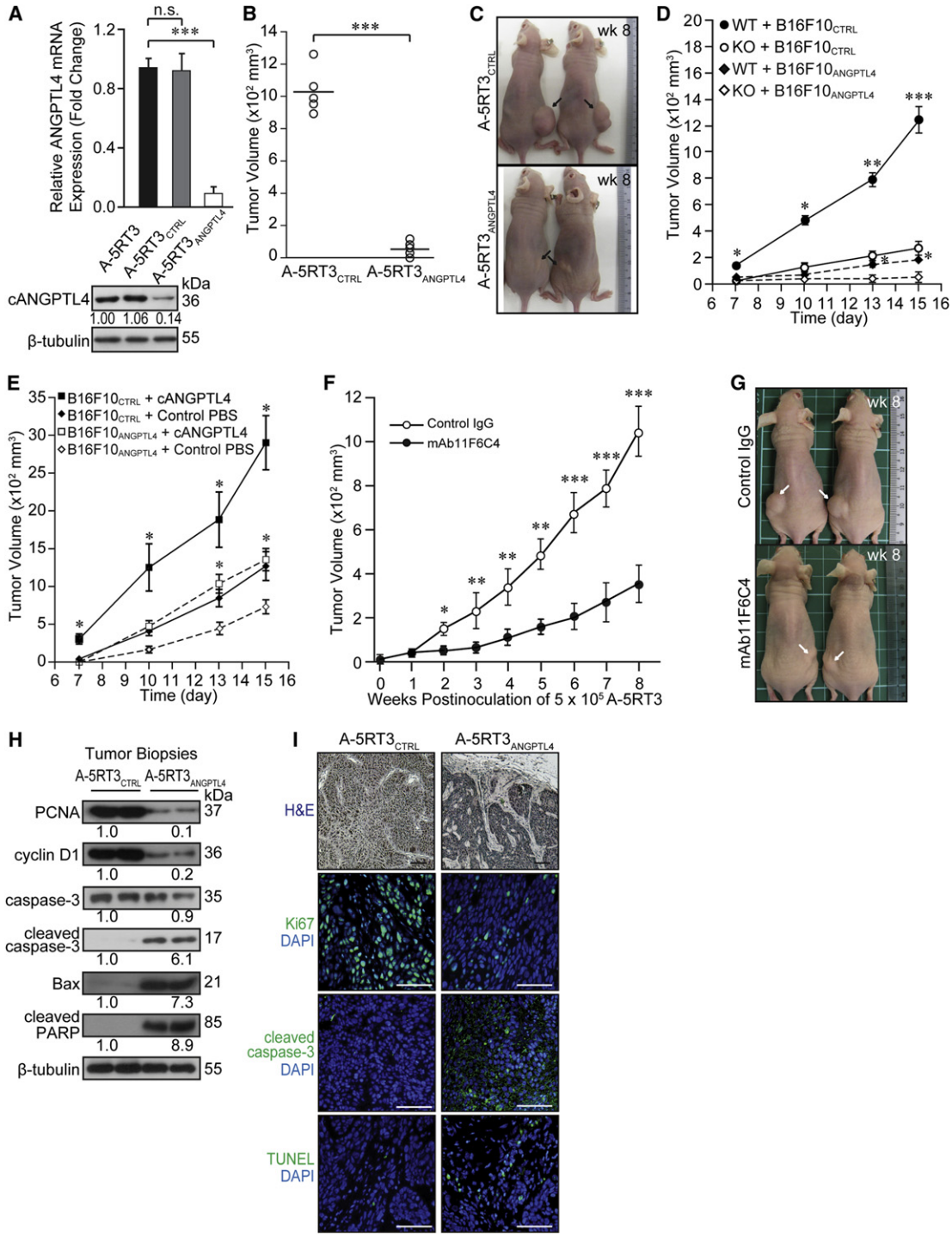

Figure 2. Suppression of ANGPTL4 Impairs Tumorigenicity

(A) Relative ANGPTL4 mRNA and protein levels in A-5RT3 (parental), A-5RT3$_{CTRL}$ (scrambled control), and A-5RT3$_{ANGPTL4}$ (knockdown) cells. Data (mean ± SD) are from three independent qPCR experiments performed in triplicate. Ribosomal protein L27 (L27) serves as a reference housekeeping gene. Immunoblot data are from three independent experiments performed in duplicate. β-Tubulin serves as a loading and transfer control.

(B) Size of xenograft tumors induced in nude mice by 5 × 10^5 of A-5RT3$_{ANGPTL4}$ or A-5RT3$_{CTRL}$ cells 8 weeks postinoculation (n = 5 per group). Each circle represents mean size from three measurements on each mouse at week 8 (wk 8).

(C) Representative pictures of A-5RT3$_{CTRL}$- and A-5RT3$_{ANGPTL4}$-induced tumors (wk 8) in (B). Black arrows indicate inoculation sites.

(D and E) Tumor volume induced in ANGPTL-KO and WT mice (D), and PBS- or recombinant cANGPTL4-treated C57BL/6J WT mice (E) by B16F10 melanoma (B16F10$_{CTRL}$, control) and ANGPTL4-knockdown (B16F10$_{ANGPTL4}$). Cells (1 × 10^6) were s.c. inoculated into each mouse (n = 6 per group). Mice (E) were treated i.v. with either 3 mg/kg of cANGPTL4 or vehicle PBS thrice a week. Values (mean ± SEM) are from three measurements of each mouse.

Suppression of ANGPTL4 Impairs Tumor Growth

Next, we investigated the biological relevance of elevated ANGPTL4 expression to tumor growth via RNAi. Four sets of siRNAs targeting different segments of the *ANGPTL4* sequence were stably introduced into the metastatic skin tumor line A-5RT3 (Mueller et al., 2001), and the subline with the highest knockdown efficiency (A-5RT3$_{ANGPTL4}$) was selected for subsequent studies. A nontargeting scrambled siRNA was also integrated into A-5RT3 (A-5RT3$_{CTRL}$) as a negative control. ANGPTL4 mRNA and protein levels were suppressed by >85% in A-5RT3$_{ANGPTL4}$ as compared with the parental A-5RT3 or A-5RT3$_{CTRL}$ (Figure 2A). The induction of interferon responses has been reported as a challenge to the specificity of some RNAi approaches (Bridge et al., 2003). To test whether the RNAi-mediated silencing of ANGPTL4 was associated with interferon responses, we measured the expression of several key interferon response genes by qPCR. No induction of *OAS1*, *OAS2*, *MX1*, or *ISGF3*γ was detected in A-5RT3$_{ANGPTL4}$ cells compared with either A-5RT3 or A-5RT3$_{CTRL}$ (Figure S2A).

As expected, the injection of A-5RT3$_{CTRL}$ cells into immunodeficient mice induced large primary tumors ($\sim$1000 mm^3) in all five mice at week 8, but A-5RT3$_{ANGPTL4}$-induced tumors displayed a 90% reduction in tumor growth (Figures 2B and 2C). A-5RT3$_{ANGPTL4}$-induced tumor growth was similarly reduced, albeit a 40% reduction, when mice were implanted with increasing number of tumor cells (Figure S2B). To strengthen the above observations, we subcutaneously (s.c.) implanted B16F10 cells into ANGPTL4-knockout (KO) and control (wild-type [WT]) mice. WT and KO mice were maintained in a C57BL/6J background, and the B16F10 melanoma was derived from the same background. Notably, B16F10 tumor cells implanted in KO mice grew slower than those implanted in WT mice; at day 15, the average tumor volume in KO mice was $\sim$6-fold less than in WT mice (Figure 2D). The injection of ANGPTL4-knockdown (B16F10$_{ANGPTL4}$) cells into KO mice induced little tumor growth and showed similar growth profile in WT mice compared to control B16F10 (B16F10$_{CTRL}$)-induced tumors in KO mice (Figure 2D). Conversely, WT mice implanted with B16F10$_{CTRL}$ cells and intravenously (i.v.) injected three times a week with recombinant N-terminal histidine-tagged cANGPTL4 showed greater tumor growth. The average tumor volume in cANGPTL4-treated mice was $\sim$3-fold larger than PBS-treated mice (Figure 2E; Figures S2C and S2D). B16F10$_{ANGPTL4}$-induced tumor growth was diminished in PBS-treated mice as compared to cANGPTL4-treated mice (Figure 2E). Next, we reasoned that treating mice injected with A-5RT3$_{CTRL}$ cells with an antibody that interferes with the action of ANGPTL4 would recapitulate the observation made with A-5RT3$_{ANGPTL4}$ cells. To this end the monoclonal human cANGPTL4-directed antibody mAb11F6C4 was identified and produced for our immunotherapy experiment based on its superior k_{on}, k_{off}, and K_D values, as determined by surface plasmon resonance (SPR) (Figure S2E and Supplemental Experimental Procedures). Notably, inhibition of ANGPTL4 with mAb11F6C4 attenuated tumor growth in immunodeficient mice, compared with control IgG-treated mice (Figures 2F and 2G). Immunoblot and IF analyses of A-5RT3$_{ANGPTL4}$-induced tumor biopsies indicated reduced cell proliferation and enhanced cell apoptosis than A-5RT3$_{CTRL}$-induced tumors (Figures 2H and 2I). A qPCR-focused array of A-5RT3$_{ANGPTL4}$-induced tumor biopsies further suggested increased expression of many pro-apoptotic genes, whereas expression of cell proliferation genes was diminished (Figure S2F and Table S1). Together, these observations clearly support a tumor-promoting role for cANGPTL4.

ANGPTL4-Deficient Tumor Cells Showed Increased Susceptibility to Anoikis

Anchorage-independent growth or anoikis resistance of tumor cells, a hallmark of tumor malignancy (Hanahan and Weinberg, 2000), was investigated by tumor colony formation in soft agar and anoikis assays (Salmon, 1984). Underscoring our in vivo findings, the colony-forming potential of A-5RT3$_{ANGPTL4}$ cells was undermined and formed fewer ($\sim$85%) tumor colonies on soft agar than A-5RT3$_{CTRL}$ (Figure 3A). Furthermore, A-5RT3$_{ANGPTL4}$ was more susceptible to anoikis, having 30% more apoptotic cells and enhanced caspase activities than A-5RT3$_{CTRL}$ cells after 2 hr of anoikis (Figures 3B and 3C). The addition of exogenous recombinant cANGPTL4 reduced the apoptotic index of A-5RT3$_{ANGPTL4}$ cells in a dose-dependent manner (Figure 3D). Similarly, ANGPTL4 deficiency in human keratinocytes rendered these cells $\sim$50% more susceptible to anoikis when compared to control keratinocytes, suggesting that a low amount of ANGPTL4 was also necessary to confer anoikis resistance in normal epithelial cells (Figure S3A). No difference in the apoptotic index was observed due to the deficiency of ANGPTL4 in adhered A-5RT3 cells or keratinocytes (Figures S3B and S3C).

ANGPTL4 Interacts with Integrins β1 and β5

The mechanism by which ANGPTL4 mediates anoikis resistance is an unanswered question. Previous studies have revealed that anoikis is an integrin-dependent process (Chiarugi, 2008; Zhan et al., 2004). Thus, we hypothesize that ANGPTL4 also exerts its role in tumor cells through integrins-mediated signaling. We examined if cANGPTL4 can interact with integrins. Indeed, SPR and ELISA results showed that ANGPTL4 specifically interacts with integrins β1 and β5, but not with β3 (Figures 3E and 3F), and these interactions were blocked by either mAb11F6C4 or

(F) Tumor volume in nude mice injected s.c. with 5 × 10^5 of A-5RT3 cells and treated i.v. with 30 mg/kg/week of either mAb11F6C4 or control IgG as a function of time (n = 6 per group). Each circle represents mean ± SEM from three measurements of each mouse.
(G) Representative pictures of control IgG- or mAb11F6C4-treated nude mice (wk 8) as described in (F). White arrows indicate inoculation sites.
(H) Immunoblot of proliferation (PCNA and cyclin D1), and apoptosis (cleaved caspase-3, Bax and cleaved PARP) markers in A-5RT3$_{ANGPTL4}$- and A-5RT3$_{CTRL}$-induced tumor biopsies. Immunoblot data are from three independent experiments performed in duplicate. β-Tubulin serves as a loading and transfer control.
(I) Hematoxylin and eosin (H&E) and IF staining of A-5RT3$_{CTRL}$- and A-5RT3$_{ANGPTL4}$-induced tumor sections. Proliferating (Ki67) and apoptotic (cleaved caspase-3 or TUNEL) cells were identified using the indicated antibodies or assay. Sections were counterstained with DAPI (blue). Scale bars represent 40 μm.
(H and I) All experiments were performed using tumor biopsies harvested from mice described in (B) and (C) at week 8 (wk 8). See also Figure S2 and Table S1.
*p < 0.05; **p < 0.01; ***p < 0.00; n.s., not significant.

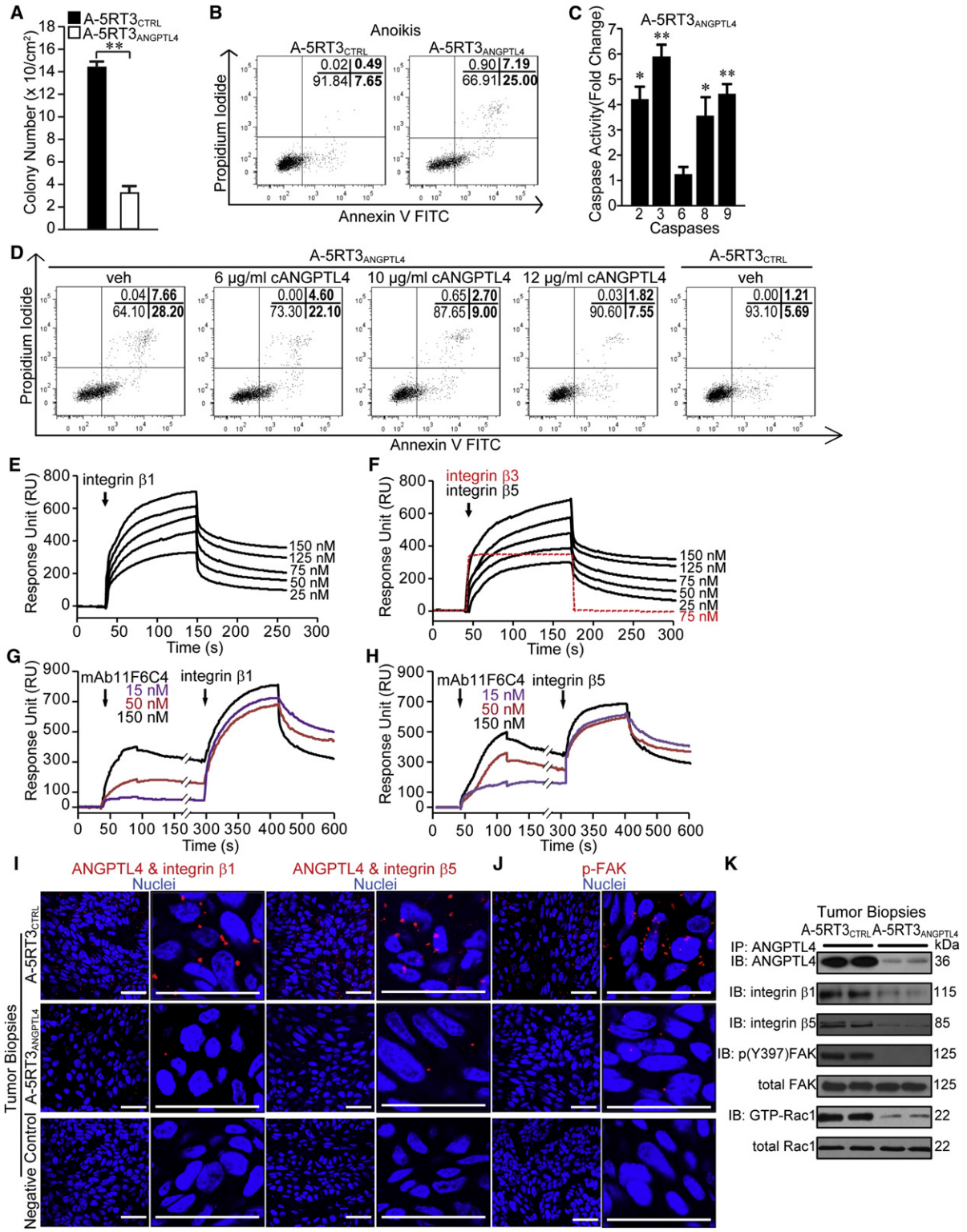

Figure 3. ANGPTL4 Interacts with Integrins β1 and β5 to Confer Tumor Cells Anoikis Resistance

(A) Quantification of A-5RT3$_{CTRL}$ and A-5RT3$_{ANGPTL4}$ tumor colonies on soft agar (left panel). Values (mean ± SD) are from four independent assays performed in triplicate. **$p < 0.01$.

(B) Percentage of apoptotic A-5RT3$_{CTRL}$ and A-5RT3$_{ANGPT4}$ cells after 2 hr of anoikis, as analyzed by FACS (5000 events). The sum of Annexin V^+/PI^- (early apoptosis) and Annexin V^+/PI^+ (late apoptosis) cells were considered apoptotic. Values (bold) denote apoptotic cells (%). Results are representative of three independent experiments.

integrin-specific antibodies (Figure 3G and 3H; Figures S3D–S3G). ANGPTL4 deficiency did not affect the expression of integrins β1, β3, and β5 (Figure S3H). An in situ proximity ligation assay (PLA) detected ANGPTL4-integrin complexes in both A-5RT3$_{CTRL}$ cells and tumors (Figure 3I; Figure S3I), confirming that this interaction also exists in vivo. Further investigation revealed that integrin activation by ANGPTL4 binding triggered focal adhesion kinase (FAK) in A-5RT3$_{CTRL}$ cells and tumors, which were reduced by >70% in A-5RT3$_{ANGPTL4}$ (Figure 3J; Figure S3J). All of these findings were corroborated by results from immunodetection of FAK on tumor biopsies (Figure 3K). Our findings suggest that ANGPTL4 secreted by epithelial tumor cells acts in an autocrine manner to hijack the integrin/FAK-regulated pathway, conferring anoikis resistance to tumors and, thus, sustaining tumor growth.

ANGPTL4 Elevates the O_2^- Level and Maintains a High O_2^-:H_2O_2 Ratio in Tumor Cells

ROS can be regulated through integrin engagement, and an elevated O_2^- level allows tumor cells to avoid anoikis (Pani et al., 2009; Pervaiz and Clément, 2007). In this regard we assessed whether ANGPTL4-integrin interaction regulates ROS production in tumor cells. Using electron paramagnetic resonance spectroscopy (EPR) in combination with 5-(diethoxyphosphoryl)-5-methyl-1-pyrroline-N-oxide (DEPMPO) spin trapping, we measured a decrease in the O_2^- level in A-5RT3$_{ANGPTL4}$ compared to A-5RT3$_{CTRL}$ cells (Figures 4A and 4B), suggesting that ANGPTL4 is vital in sustaining O_2^- production in tumor cells. To determine the source of O_2^-, similar experiments were performed using specific inhibitors that block the mitochondrial respiratory chain complex I and membrane-bound NADPH oxidase, which are two major producers of O_2^- in mammalian cells (Giannoni et al., 2008). Treatment of tumor cells with rotenone, a mitochondrial respiratory chain complex I inhibitor (Irani et al., 1997), did not alter cellular O_2^- level (Figures 4A and 4B), suggesting that this complex has little role in generating O_2^- in tumors. Further excluding mitochondria as the source of ANGPTL4-mediated O_2^- generation, qPCR analysis showed no change in the expression of selected genes in the methionine/homocysteine metabolic cycle (Figure S4A), as previously studied in diabetic rodent hepatocytes (Wang et al., 2007). In contrast the O_2^- level was abrogated by using two different NADPH oxidase inhibitors (Ushio-Fukai and Nakamura, 2008), diphenylene iodonium (DPI) and apocynin (Figures 4A and 4B). ROS generated through the involvement of the small GTPase Rac1 and NADPH oxidase upon integrin engagement exert a mandatory role in transmitting a prosurvival signal that ensures that tumor cells escape from anoikis (Giannoni et al., 2008; Jonesson and Bar-Sagi, 1998). Comparative immunoblot analyses of anti-cANGPTL4 immunoprecipitates from A-5RT3$_{CTRL}$- and A-5RT3$_{ANGPTL4}$-induced tumor lysates detected integrins β1 and β5, along with phosphorylated FAK and active GTP-bound Rac1, in A-5RT3$_{CTRL}$-induced tumors, all of which were reduced in A-5RT3$_{ANGPTL4}$-induced tumors (Figure 3K). To further validate the relevance of Rac1 in ANGPTL4-mediated O_2^- production, we transiently transfected A-5RT3$_{CTRL}$ and A-5RT3$_{ANGPTL4}$ cells with dominant-negative Rac1 (T17N) and constitutively active Rac1 (G12V), respectively. We measured a diminished O_2^- level in the former and, conversely, an obviously rescued O_2^- production in the latter. The percentage of inhibition and recovery was consistent with the ~65% transfection efficiencies, as estimated using a GFP-expressing vector. The requirement of Rac1 suggested a Rac1-engaged Nox (i.e., Nox1-3)-dependent mechanism for O_2^- production. Because Nox 3 is expressed predominantly in the inner ear (Paffenholz et al., 2004), we examined the expression of Nox1 and Nox2 in A-5RT3 (Figure S4B). Next, we performed Nox1 and Nox2 knockdown (Nox1 kd and Nox2 kd, respectively) in A-5RT3$_{CTRL}$ and A-5RT3$_{ANGPTL4}$ cells (Figure S4C), and measured the O_2^- level using EPR (Figures 4A and 4B). Results indicated that Nox1 NADPH oxidase is the predominant source of ANGPTL4-mediated O_2^- generation in tumor cells. The O_2^- level was completely abolished by superoxide scavenger Tiron, which serves as a negative control for superoxide measurements (Figures 4A and 4B). These data were reproduced by a chemiluminescence assay using 2-methyl-6-(4-methoxyphenyl)-3, 7-dihydroimidazo[1,2-a]pyrazin-3-one hydrochloride (MCLA) (Figure 4C) (Münzel et al., 2002). Next, we measured the level of H_2O_2 in tumor cells in the presence of a specific catalase inhibitor, 3-amino-l, 2, 4-triazole (Chance et al., 1979; Wagner et al., 2005). H_2O_2 levels were higher in A-5RT3$_{ANGPTL4}$ than A-5RT3$_{CTRL}$ cells (Figure 4D). Nox1 kd did not affect the H_2O_2 level, suggesting that ANGPTL4 modulated H_2O_2 production, linked to an unknown mechanism (Figure S4D). Notably, the lower O_2^- level and O_2^-:H_2O_2 ratio were concurrent with 3-fold more apoptosis and enhanced caspase activities within 2 hr of anoikis in A-5RT3$_{ANGPTL4}$ compared

(C) Relative activities of caspases 2, 3, 6, 8, 9 in A-5RT3$_{ANGPTL4}$ cells compared to A-5RT3$_{CTRL}$ cells (assigned value of one) after 2 hr of anoikis. Values (mean ± SD) are from three independent experiments performed in triplicate. *$p < 0.05$; **$p < 0.01$.

(D) Percentage of anoikis-induced apoptotic A-5RT3$_{ANGPT4}$ cells in the presence of increasing exogenous recombinant cANGPTL4, as analyzed by FACS (5000 events). Vehicle (PBS)-treated A-5RT3$_{CTRL}$ and A-5RT3$_{ANGPT4}$ cells served as controls for comparison. The apoptotic index is described in (B).

(E and F) Representative sensorgrams of three independent experiments showing binding profiles between immobilized-ANGPTL4 and integrin β1 (E) or integrin β5 (F). Integrin β3 (75 nM) did not show any detectable interaction (F, dotted red line). Sensorgrams were corrected against a reference flow cell with no immobilized protein. $K_D \sim 10^{-7}$ M was determined after global fitting (Langmuir 1:1 model) using Scrubber2.

(G and H) Representative sensorgrams showing dose-dependent blocking of integrin β1 (G) and integrin β5 (H) to immobilized-ANGPTL4 by preinjection with the indicated concentrations of mAb11F6C4.

(I and J) In situ PLA detection of ANGPTL4:integrin β1 (I, left two panels), ANGPTL4:integrin β5 (I, right two panels), and phosphorylated FAK (J) in A-5RT3$_{ANGPTL4}$- and A-5RT3$_{CTRL}$-induced tumor biopsies. Higher magnification images are shown (I, second and fourth panels; J, right panel). PLA signals are shown in red, and nuclei are stained blue by Hoechst dye. Negative controls were performed with only anti-nANGPTL4 (I) or anti-FAK (J) antibodies. Scale bars represent 40 μm.

(K) Immunoprecipitation and immunodetection of ANGPTL4, integrin β1, integrin β5, total FAK, phosphorylated FAK (pY397FAK), total Rac1, and GTP-bound Rac1 (GTP-Rac1) from the indicated tumor sections. A configuration-specific monoclonal anti-Rac-GTP antibody was used for immunoprecipitation of GTP-Rac1. Total FAK serves as a loading and transfer control.

Experiments in (I)–(K) were performed using tumor biopsies described in Figures 2B and 2C. All experiments in (B)–(K) were repeated three times with consistent results. See also Figure S3.

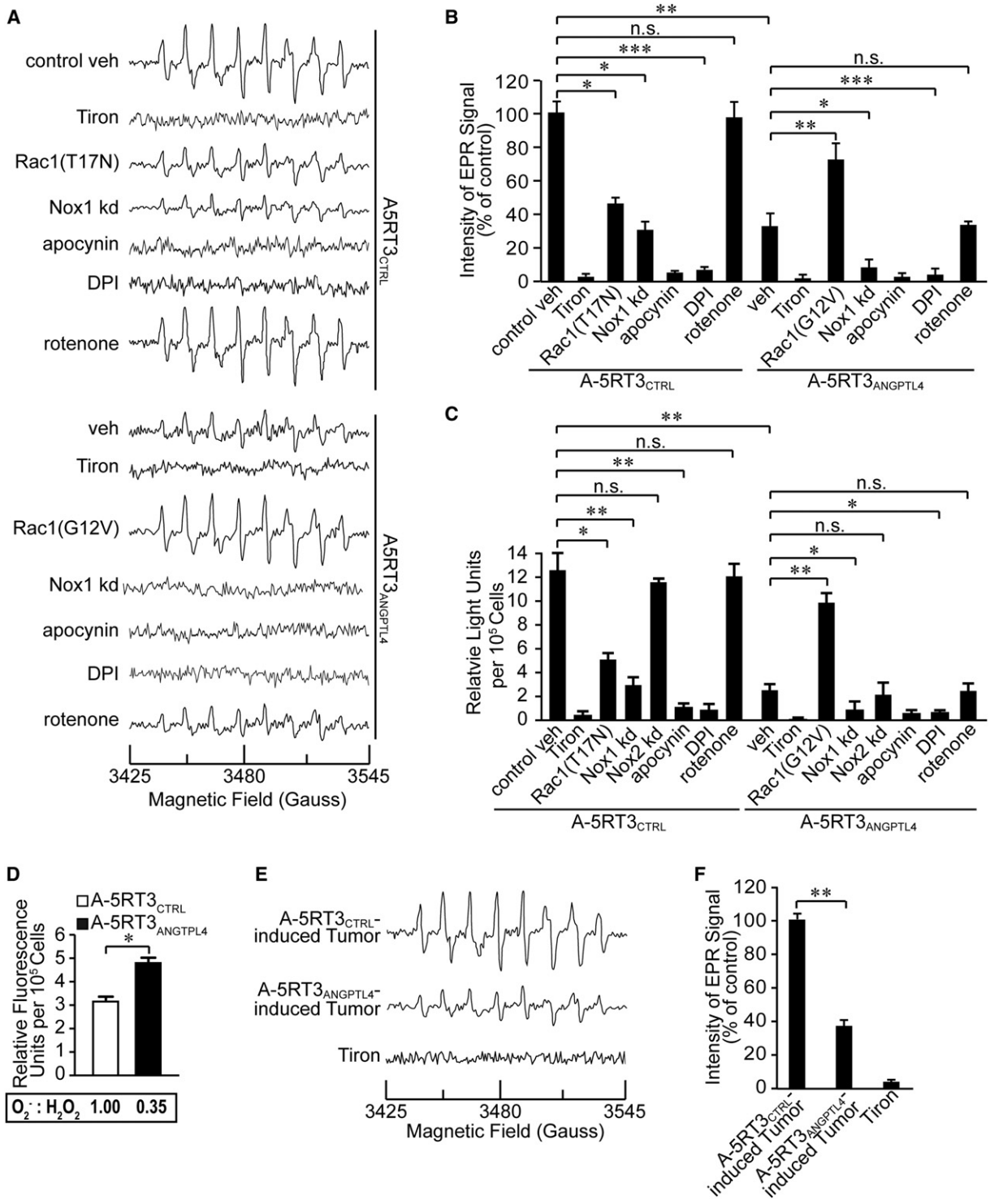

Figure 4. ANGPTL4 Elevates O_2^- Level and Maintains a Relatively High O_2^-:H_2O_2 Ratio in Tumor Cells

(A and E) Representative EPR spectra of DEPMPO-superoxide spin adduct from A-5RT3$_{CTRL}$ and A-5RT3$_{ANGPTL4}$ cells (A) or A-5RT3$_{CTRL}$- and A-5RT3$_{ANGPTL4}$-induced tumors (E) in the absence or presence of indicated chemicals or inhibitors. A-5RT3$_{CTRL}$ and A-5RT3$_{ANGPTL4}$ cells were transiently transfected either with vector expressing Rac1(T17N) or Rac1(G12V), or with ON-TARGETplus siRNA against either Nox1 (Nox1 kd) or Nox2 (Nox2 kd). The superoxide adduct of DEPMPO has hyperfine splitting constants of: a_N = 13.13 gauss; a_P = 55.61 gauss; a^{β}_H = 13.11 gauss; and a^{γ}_H = 0.71, 0.42, 0.7, 0.25, and 0.6 gauss.

(B and F) EPR signal intensity at 3480 gauss from A-5RT3$_{CTRL}$ and A-5RT3$_{ANGPTL4}$ cells in (A) or tumors in (E).Tiron-treated measurements serve as negative signal controls.

(C) Measurement of O_2^- levels using the MCLA assay in A-5RT3$_{CTRL}$ and A-5RT3$_{ANGPTL4}$ cells in the absence or presence of the indicated chemicals or inhibitors.

to A-5RT3$_{CTRL}$ cells (Figures 3B, 3C, and 4A–4D). Accordingly, we observed a reduced O_2^- level in A-5RT3$_{ANGPTL4}$-induced tumors compared to A-5RT3$_{CTRL}$-induced tumors (Figures 4E and 4F), which was associated with increased apoptosis (Figure 2H and 2I; Figure S2F).

To underscore the relevance of these findings to other cancers, similar experiments were performed using the breast cancer line MDA-MB-231, after using mAb11F6C4 to dose dependently neutralize endogenous cANGPTL4. We showed earlier that mAb11F6C4 was able to block cANGPTL4-integrin interaction (Figures 3G and 3H; Figures S3D–S3G). Consistent with the above results, the inhibition of cANGPTL4 in MDA-MB-231 reduced the O_2^- level (Figures S4E–S4G), lowered the O_2^-:H_2O_2 ratio (Figure S4H), and enhanced apoptosis and caspase activities (Figures S4I and S4J). Nox1 kd (Figure S4K) but not Nox2 kd reduced ANGPTL4-mediated O_2^- production (Figures S4E–S4G) with little effect on H_2O_2 production (Figure S4L). Together, these findings indicate that ANGPTL4 protects tumor cells from anoikis via an NADPH oxidase-dependent O_2^- generation mechanism.

ANGPTL4-Mediated O_2^- Activates the Src, PI3K/PKBα, and ERK Survival Pathways

Previous reports have shown that ROS produced via integrin engagement oxidizes and activates Src, which stimulates the ERK and PKBα prosurvival pathways (Giannoni et al., 2008, 2009; Pani et al., 2009). Both pathways regulate the subcellular localization or stability of BH3-only apoptotic proteins (e.g., Bad and Bim), which are essential for executing anoikis (Bouillet and Strasser, 2002). Thus, we asked whether ANGPTL4-integrin engaged O_2^- generation employs these downstream signaling pathways to modulate tumor cell behavior. Immunoblot analyses revealed diminished expression of oxidized/activated Src, phosphorylated PKBα, and ERK1 in A-5RT3$_{ANGPTL4}$-induced tumors and A-5RT3$_{ANGPTL4}$ cells (Figure 5A, and left panel of Figure 5B). Similar immunoblot analyses performed in the presence of DPI and with Nox1 kd cells revealed reduced Src, PKBα, and ERK1 activation, emphasizing the role of O_2^- in their activities (Figure 5B). The inhibition of PI3K by LY294002 and Wortmannin, a pivotal upstream mediator of PKBα, caused 4-fold more apoptosis of tumor cells upon anoikis challenge, reaching levels comparable to those of A-5RT3$_{ANGPTL4}$ cells (Figure 5C). In addition, inhibition of MEK1/2, the upstream signal of ERK1, by PD98059 also resulted in an enhancement of apoptotic cell numbers, albeit to a lesser extent (~50%) compared to PI3K inhibitors (Figure 5C). These results suggest that the PI3K/PKBα and ERK1/2 downstream survival pathways are modulated and exploited by ANGPTL4 engagement in tumor cells, the former being the predominant pathway.

The 14-3-3 adaptor protein is known to act downstream of the aforementioned survival pathways by sequestering pro-apoptotic Bad from the mitochondria to prevent apoptosis (She et al., 2005). In agreement with these previous findings, the number of 14-3-3/Bad complexes and 14-3-3β/σ proteins was reduced by ~70% in A-5RT3$_{ANGPTL4}$-induced tumors (Figures 5D–5F). The Na^+/H^+ exchanger 1 (NHE), which positively influences cell proliferation by maintaining an alkaline intracellular environment (Akram et al., 2006), was also diminished in A-5RT3$_{ANGPTL4}$-induced tumors (Figure 5D), indicating that NHE plays a subsidiary role in ANGPTL4-mediated tumor cell growth. Upon oxidant challenge in tumor cells, the induction of superoxide dismutase (SOD) expression is muted, allowing tumor cell proliferation (Oberley, 2001; Pervaiz and Clément, 2007). Indeed, we found that cytosolic Zn/CuSOD expression was enhanced in A-5RT3$_{ANGPTL4}$-induced tumors (Figure 5D), which contribute to a reduced O_2^-:H_2O_2 ratio via an indirect but linked mechanism (Figure 4D).

ANGPTL4 Deficiency Abrogates O_2^- Production and Sensitizes Cancer Cells to Anoikis

Our results revealed that the suppression of ANGPTL4, either by RNAi (Figures 4A–4C) or inhibition with mAb11F6C4 (Figures S4E–S4G), results in a dose-dependent reduction of O_2^- levels. To underscore the importance of ANGPTL4 in the regulation of O_2^- production, maintenance of a high O_2^-:H_2O_2 ratio, and, hence, tumor survival, we examined the impact of reduced ANGPTL4 on anoikis in nine different cancer cell lines, in addition to A-5RT3 and MDA-MB-231 cells. Treatment with mAb11F6C4 resulted in a dose-dependent reduction of O_2^- levels (40%–80% for 6 μg/ml mAb11F6C4) (Figure 6A; Figure S5A), a reduction in the O_2^-:H_2O_2 ratio (70%–90% for 6 μg/ml mAb11F6C4) (Figure 6B; Figure S5B), a 3- to 8-fold increase in the caspase activities (Figure 7A; Figure S6A), and 30%–60% more apoptotic tumor cells (Figure 7B; Figure S6B), all indicating weakened anoikis resistance. A higher percentage of apoptotic tumor cells was also observed using inducible RNAi against ANGPTL4 in the MDA-MB-231 line (Figure S6C). These findings indicate that ANGPTL4-mediated O_2^- production for anoikis resistance may be a common feature in tumor cells. Taken together, our study showed that tumor-secreted ANGPTL4 interacted with integrins in an autocrine fashion to stimulate NADPH oxidase-dependent generation of O_2^-, promoting a high O_2^-:H_2O_2 ratio, and consequently activating downstream PI3K/PKBα and ERK activities (Figure 8).

DISCUSSION

The loss of dependence on integrin-mediated ECM contact for growth (i.e., anoikis resistance) is an essential feature of tumor cells, but the mechanism by which anoikis resistance is acquired is a central problem in cancer biology. Our findings demonstrated that ANGPTL4-mediated integrin engagement activates ROS production, which leads to a prosurvival signal and sustained anchorage-related signals even in the absence of ECM and cell-cell contact. We showed that cANGPTL4 was detected and elevated in many human tumor cells and was predominantly secreted by proliferative tumor epithelial cells. cANGPTL4 specifically binds to integrins β1 and β5 on tumor cells and

(D) Measurement of H_2O_2 levels using the Amplex red assay in A-5RT3$_{CTRL}$ and A-5RT3$_{ANGPTL4}$ cells. Arbitrary relative O_2^-:H_2O_2 ratios are shown in boxes.
(B–D and F) Values were normalized to total proteins and presented as mean ± SEM. Data are from three independent experiments performed in triplicate.
*$p < 0.05$; **$p < 0.01$; ***$p < 0.001$; n.s., not significant.
Vehicle-treated A-5RT3$_{CTRL}$ cells (B and C) and A-5RT3$_{CTRL}$-induced tumor (F) serve as cognate controls. See also Figure S4.

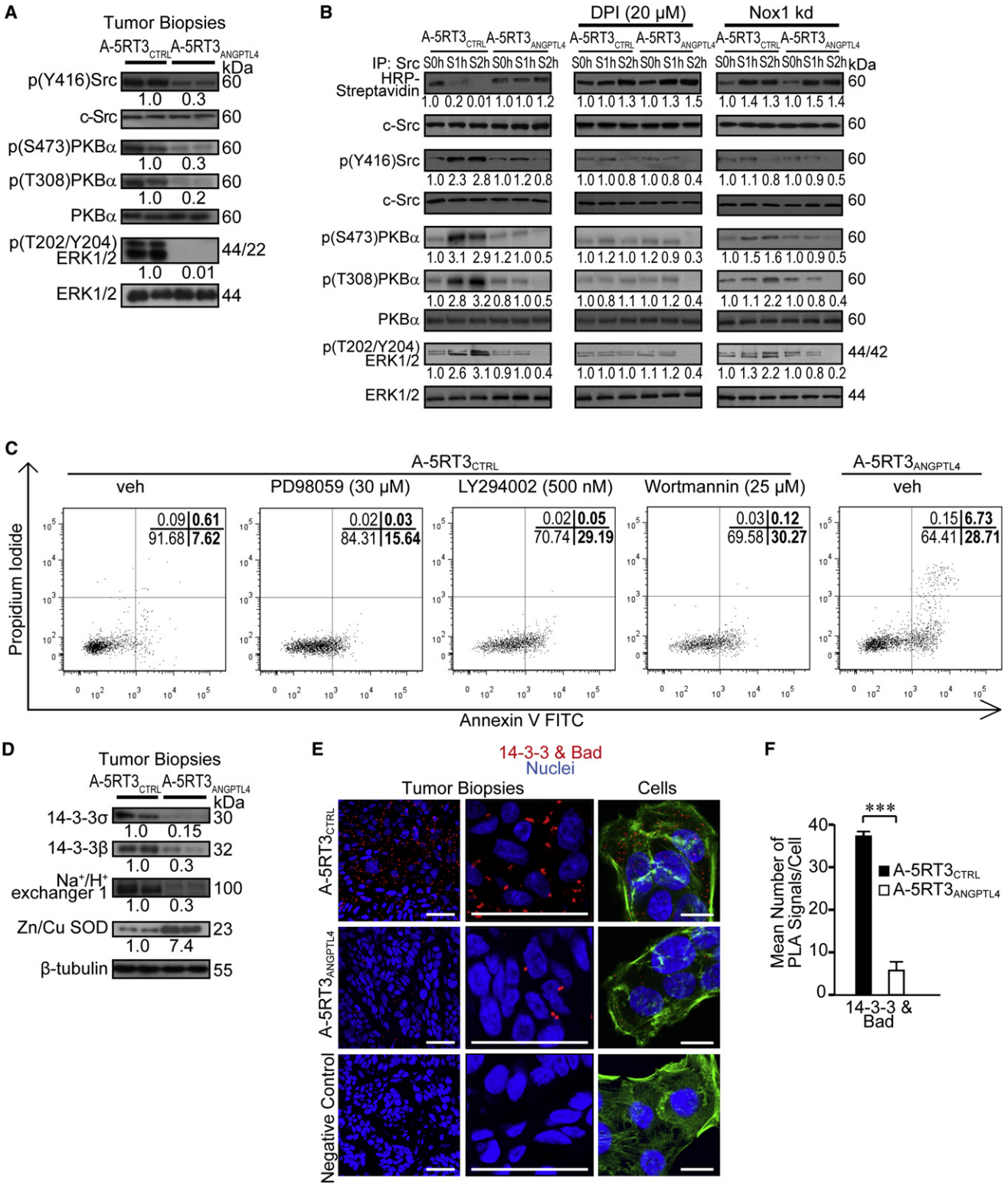

Figure 5. ANGPTL4-Mediated O_2^- Regulates Src and Promotes the PI3K/PKBα and ERK Survival Pathways

(A and D) Immunoblot of the indicated proteins in A-5RT3$_{ANGPTL4}$- and A-5RT3$_{CTRL}$-induced tumor biopsies. Values are mean from four independent experiments. c-Src (A) and β-tubulin (D) serve as loading and transfer controls, respectively.

(B) Immunoblot of the indicated proteins in A-5RT3$_{ANGPTL4}$ and A-5RT3$_{CTRL}$ cells in the absence or presence of 20 μM DPI, and in Nox1 kd A-5RT3$_{ANGPTL4}$ and A-5RT3$_{CTRL}$ cells. Cells were suspended for 0, 1, and 2 hr (S0h, S1h, and S2h, respectively). Cell lysates were labeled with 100 μM *N*-(biotinoyl)-*N*′-(iodoacetyl)

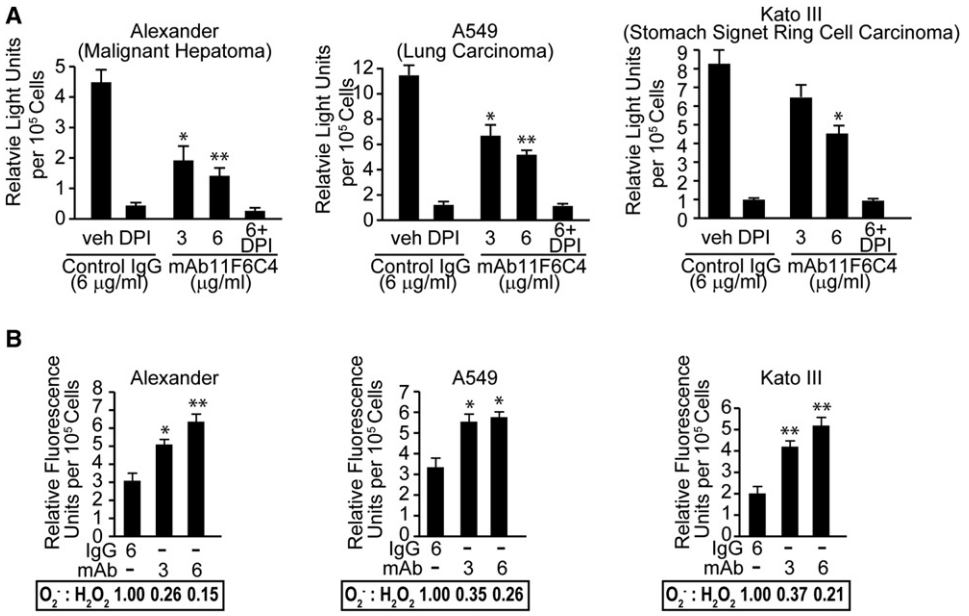

Figure 6. ANGPTL4 Maintains a Relatively High O_2^-:H_2O_2 Ratio in Tumor Cells

Measurement of O_2^- (A) and H_2O_2 (B) levels in three different tumor lines by MCLA assay and Amplex red assay, respectively. H_2O_2 was measured in the presence of the specific catalase inhibitor, 3-amino-l, 2, 4-triazole. Arbitrary relative O_2^-:H_2O_2 ratios (B) are shown in boxes. Values (mean ± SD) are normalized to the total protein content. Three independent experiments were performed with consistent results. *$p < 0.05$; **$p < 0.01$. See also Figure S5.

activates FAK and Rac1, which further stimulates NADPH oxidase-mediated O_2^- production via an autocrine pathway. However, it is conceivable that in tissues/organs, expressing high levels of cANGPTL4 in proximity to the tumor site may transmit a paracrine signal. Although integrins alone are not oncogenic, integrin-mediated signaling is often required to enable tumor survival and influence tumor growth (Desgrosellier and Cheresh, 2010). The pro-oxidant intracellular environment led to redox-mediated activation of the Src machinery and, therefore, stimulated downstream PI3K/PKBα and ERK prosurvival pathways. This further triggered the 14-3-3 adaptor protein to sequester the pro-apoptotic Bad protein from mitochondria, conferring resistance to anoikis and favoring tumor survival and growth.

The dysregulation of intracellular ROS levels, resulting in an excessive level or persistent elevation of ROS, has been linked to tumor growth, invasiveness, and metastasis. Indeed, elevated levels of ROS are detected in almost all cancers (Liou and Storz, 2010). An elevated O_2^- or O_2^-:H_2O_2 ratio is particularly important for cancer cells to sustain their tumorigenicity and metastatic potential (Clément and Pervaiz, 2001; Pervaiz and Clément, 2007). We found that the disruption of ANGPTL4-mediated redox signaling via genetic and antibody-mediated suppression of ANGPTL4 essentially reduced the activities of FAK, Rac1, and O_2^- production. These changes resulted in an increase in tumor cells' sensitivity to anoikis and impaired tumorigenesis. ANGPTL4-stimulated NADPH oxidase activity, leading to O_2^- production, can be inhibited NADPH oxidase inhibitors, but not by the mitochondrial complex I inhibitor rotenone. This suggests that O_2^- was "purposely" and enzymatically produced by NADPH oxidase, rather than as a by-product of mitochondrial activity. Two survival pathways, the PKBα and ERK, which have been shown to exert anoikis-suppressing effects (Westhoff and Fulda, 2009; Zhan et al., 2004), were complementarily employed by ANGPTL4 to confer resistance to anoikis in tumor cells.

The tumor-promoting role of inflammation in the tumor microenvironment is well recognized (Aggarwal and Gehlot, 2009). PPARγ and δ/β play major roles in the regulation of inflammation and are implicated in tumorigenesis (Peters and Gonzalez, 2009; Murphy and Holder, 2000). Although no correlation between the expression of either PPARγ or δ/β, and their target gene ANGPTL4, was observed in our analysis of PNSs and SCCs,

ethylenediamine to evaluate the Src redox state. An HRP-Streptavidin immunoblot performed on the anti-Src immunoprecipitate showing reduced Src. The immunoprecipitate was probed with anti-c-Src for normalization. Values (mean ± SD) represent the mean fold change against the value at S0h. Data shown are representatives of three independent experiments.

(C) Percentage of apoptotic A-5RT3$_{ANGPTL4}$ and A-5RT3$_{CTRL}$ cells, treated with either MEK inhibitor PD98059 or PI3K inhibitors LY294002 and Wortmannin, after 2 hr of anoikis challenge and analyzed by FACS (5000 events). Apoptotic index as described in Figure 3B. Sum of Annexin V^+/PI^- and Annexin V^+/PI^+ cells were considered apoptotic. Values are mean from three independent experiments.

(E) In situ PLA detection of 14-3-3:Bad complexes in indicated tumor sections and cells. PLA signals are red dots, and Hoechst-stained nuclei are in blue. Cells were counterstained with Alexa 488-phalloidin for actin stress fibers (green). Negative controls were performed with only anti-14-3-3 antibodies. Data shown are representative of three independent experiments. Scale bars represent 40 μm.

(F) Number (mean ± SD) of 14-3-3:Bad complexes (E, right panel) was calculated from 200 cells (n = 3; 600 cells total) using BlobFinder software. ***$p < 0.001$.

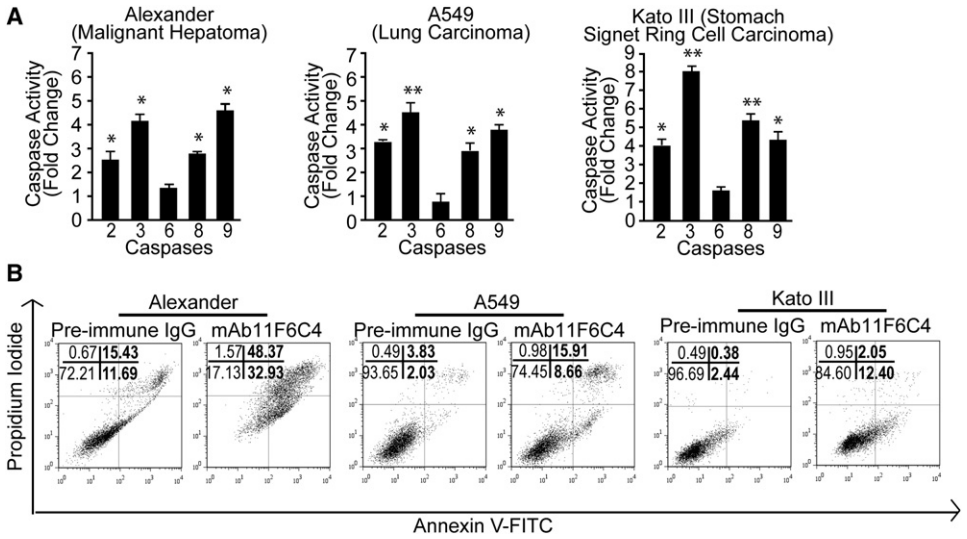

Figure 7. Deficiency of ANGPTL4 Activates Caspase Activities and Induces Apoptosis upon Anoikis in Tumor Cells

(A) Relative activities of caspases 2, 3, 6, 8, and 9 were measured after 2 hr of anoikis. Fold increase of caspase activities in mAb11F6C4 (6 μg/ml)-treated cells was calculated by comparing with the caspase activities of cells treated with preimmune IgG (6 μg/ml). Values (mean ± SD) are from three independent experiments with consistent results.*$p < 0.05$; **$p < 0.01$.

(B) Percentage of apoptotic cells in three tumor lines after 2 hr of anoikis as analyzed by FACS (5000 events). Tumor cells were treated with 10 μg/ml of control IgG or mAb11F6C4. Apoptotic index is as described in Figure 3B. Results are mean from three independent experiments. $p < 0.05$. See also Figure S6.

we cannot exclude their involvement and/or other oncogenic pathways or cell types in the tumor microenvironment, which enhanced the expression of cANGPTL4 in tumors. It is also conceivable that PPARs in cancer-associated fibroblasts play a more dominant role in the regulation of epithelial tumor growth. Indeed, PPARβ/δ-deficient fibroblasts can increase the proliferation of normal epithelial cells and SCCs via regulation of the interleukin-1 signaling pathway (Chong et al., 2009). A dysregulated inflammatory response promotes tumorigenesis and malignancy by stimulating ROS production (Aggarwal and Gehlot, 2009). Although not examined in this study, we cannot rule out the possibility that other mechanisms to produce O_2^-, such as cytosolic 5-lipooxygenase, may act in conjunction with ANGPTL4-stimulated NADPH oxidase activity to maintain an elevated intracellular O_2^- level for tumor growth (Chiarugi and Fiaschi, 2007). Despite inconclusive findings from clinical trials on the effect of antioxidants on cancer (Blot et al., 1993; Omenn et al., 1994; Hennekens et al., 1996; Lee et al., 1999), our findings that the specific inhibition of ANGPTL4-mediated integrin signaling and intracellular O_2^- production induce tumor cell apoptosis suggest that anticancer therapeutics focusing on redox-based apoptosis induction remain an exciting and viable strategy.

EXPERIMENTAL PROCEDURES

Human Tumor Samples

Human BCC biopsies and SCC biopsies along with their paired PNSs were provided by J.Y.P., S.H.T., and purchased from USA Asterand, plc., Detroit, MI. BCC samples, SCC samples, and PNSs, inclusive of epithelia and stroma, were subjected to protein and RNA extraction for immunoblotting and qPCR analyses, respectively. The study was approved by National Healthcare Group Domain-Specific Review Boards (NHG-DSRB). All the tumor samples had been de-identified prior to the analyses.

Tumorigenicity Assay

BALB/c athymic nude female mice (20–22 g), aged 5–6 weeks, and WT C57BL/6J female mice (20–25 g), aged 6–8 weeks, were purchased from A*STAR Biological Resources Centre (Singapore). C57BL/6J female WT and ANGPTL4-KO mice were used (Koster et al., 2005). The animal studies were approved and carried out in compliance with the regulation from Institutional Animal Care and Use Committee (IACUC0092), NTU. For nude mice experiments, 5×10^5 cells (A-5RT3$_{CTRL}$ or A-5RT3$_{ANGPTL4}$) were injected s.c. into the interscapular region of each nude mouse (n = 5). The injection site was rotated to avoid site bias. The injected tumor cells were allowed to grow for 8 weeks. The xenograft tumors were externally measured with a Vernier caliper every other day, and tumor volume was estimated using the equation: $V = (L \times W^2)/2$, where L and W are the length of the major and minor axis of the tumor, respectively. To test the effect of the number of injected cells on tumorigenicity, nude mice were inoculated with 0.5 ×, 2 ×, and 8 × 10^6 A-5RT3$_{CTRL}$ or A-5RT3$_{ANGPTL4}$ cells as above. Experiments were terminated at week 4 according to IACUC protocol because tumor volume in the 8 × 10^6 inoculation group approached 3000 mm^3.

For the antibody treatment, nude mice (n = 6) were implanted with A-5RT3 as above. One week postimplantation, 30 mg/kg/week of either mAb11F6C4 or isotype control IgG was i.v. administered for 4 weeks. The dose of antibody and delivery mode were consistent with studies using mAb14D12, another anti-ANGPTL4 mAb27 (Desai et al., 2007). KO mice and cANGPTL-treated C57BL/6J mice studies were performed as previously described (Sun and Lodish, 2010). Briefly, 1 × 10^6 B16F10$_{CTRL}$ (scrambled control) or B16F10$_{ANGPTL4}$ (ANGPTL4 knockdown) cells were s.c. injected into the interscapular region of the indicated mice (n = 4–6). Mice were i.v. treated with either 3 mg/kg of cANGPTL4 or control PBS three times a week. Animals were monitored and tumor volumes measured as above. Mice were sacrificed at the end of the experiment, and tumors were harvested for further analyses.

In Situ PLA

Duolink in situ PLA (Olink Bioscience) was performed on tumor biopsies or cells as described (Tan et al., 2009). The paired-primary antibodies used in the present study were rabbit anti-p(Y397)FAK and mouse anti-FAK antibodies, rabbit anti-pan-14-3-3 and mouse anti-BAD antibodies, and mouse anti-cANGPTL4 with either rabbit anti-β1, β3, or β5 integrin antibodies. As a

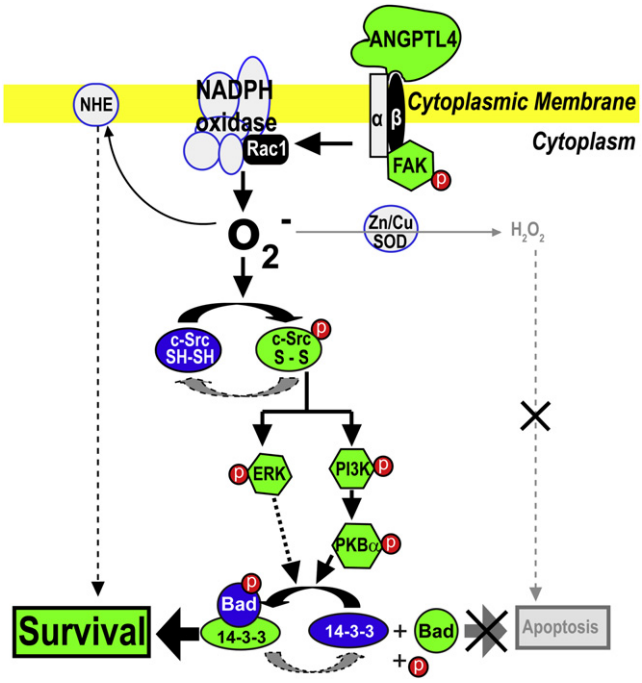

Figure 8. ANGPTL4-Mediated Regulation of O_2^- Production in Tumors

In an autocrine manner, tumor-derived ANGPTL4 specifically binds to integrins β1 or β5 and subsequently activates FAK and Rac1 activities, which further activates the NADPH oxidase-dependent generation of "*onco-ROS*" O_2^-, promoting a relatively high O_2^-:H_2O_2 ratio in tumor cells. This pro-oxidant intracellular milieu, which may subsidiarily be maintained through NHE, favors cell survival and proliferation by oxidizing/activating the Src machinery and, therefore, stimulates its downstream PI3K/PKBα- and ERK-mediated survival pathways. This further triggers the 14-3-3 adaptor protein to sequester pro-apoptotic Bad from mitochondria to prevent apoptosis and favor cell survival.

negative control, PLA was performed using only anti-FAK, anti-pan-14-3-3, or anti-nANGPTL4 antibodies, respectively. Briefly, sections/cells were fixed with 4% paraformaldehyde for 15 min. The slides were washed twice with PBS, blocked for 1 hr at room temperature with 2% BSA in PBS containing 0.1% Triton X-100, followed by incubation with the indicated antibody pairs overnight at 4°C. PLA was performed as recommended by the manufacturer. Images were taken using an LSM710 confocal laser scanning microscope with a Plan-Apochromat 63×/1.40 Oil objective and ZEN 2008 software (Carl Zeiss).

Measurement of O_2^- and H_2O_2

Production of O_2^- from tumor cells was measured using an O_2^--sensitive luciferin derivative, MCLA (Invitrogen). Cells (5×10^4) were trypsinized, washed, lysed in Krebs buffer, and treated either individually or combinatorially for 0.5 hr with the following chemicals: 10 mM Tiron, 20 μM diphenyleneiodonium chloride (DPI) or 500 μM apocynin, 50 μM rotenone, and 3 or 6 μg/ml monoclonal human anti-cANGPTL4 antibody mAb11F6C4. MCLA (2 μM) was added, and the luminescent signal was recorded immediately thereafter for 1 min with a GloMax 20/20 Luminometer (Promega). Intracellular H_2O_2 was measured as previously described (Wagner et al., 2005). We performed two control experiments to verify that we were measuring H_2O_2. The specificity of the assay for H_2O_2 was verified with catalase, and the degradation of H_2O_2 or inhibition of the assay system by the sample was analyzed by determining the recovery of exogenously added H_2O_2. The fold change in the O_2^-:H_2O_2 ratio of A-5RT3$_{ANGPTL4}$ and mAb11F6C4-treated tumor cells was determined by direct comparison with the value of either A-5RT3$_{CTRL}$ or control IgG-treated tumor cells, which were arbitrarily assigned the value of one.

Statistical Analyses

Statistical significance between two groups was analyzed using unpaired nonparametric test (Mann-Whitney test) or with a Student's t test (SPSS, Inc.). All statistical tests were two sided. A p value of ≤ 0.05 was considered significant.

SUPPLEMENTAL INFORMATION

Supplemental Information includes Supplemental Experimental Procedures, six figures, and one table and can be found with this article online at doi:10.1016/j.ccr.2011.01.018.

ACKNOWLEDGMENTS

This work was supported by grants from Ministry of Education, Singapore (ARC18/08), Nanyang Technological University (RG127/05, RG82/07), and Biomedical Research Council (10/1/22/19/644) to N.S.T.; a grant from the German Research Aid (Deutsche Krebshilfe: Tumorstammzellverbund) to P.B. We thank Dr. Samuel Ko and Anna Teo (Carl Zeiss, Singapore Pte Ltd.) for their expertise in laser capture microdissection with PALM Microbeam Axio Observer Z1 and image acquisition using LSM710 confocal microscope and MIRAX MIDI. The authors declare that they have no competing financial interests.

Received: July 5, 2010
Revised: November 11, 2010
Accepted: January 4, 2011
Published: March 14, 2011

REFERENCES

Aggarwal, B.B., and Gehlot, P. (2009). Inflammation and cancer: how friendly is the relationship for cancer patients? Curr. Opin. Pharmacol. *9*, 351–369.

Akram, S., Teong, H., Fliegel, L., Pervaiz, S., and Clément, M. (2006). Reactive oxygen species-mediated regulation of the Na^+-H^+ exchanger 1 gene expression connects intracellular redox status with cells' sensitivity to death triggers. Cell Death Differ. *13*, 628–641.

Belanger, A.J., Lu, H., Date, T., Liu, L.X., Vincent, K.A., Akita, G.Y., Cheng, S.H., Gregory, R.J., and Jiang, C. (2002). Hypoxia up-regulates expression of peroxisome proliferator-activated receptor γ angiopoietin-related gene (PGAR) in cardiomyocytes: role of hypoxia inducible factor 1α. J. Mol. Cell. Cardiol. *34*, 765–774.

Blot, W.J., Li, J.Y., Taylor, P.R., Guo, W., Dawsey, S., Wang, G.Q., Yang, C.S., Zheng, S.F., Gail, M., Li, G.Y., et al. (1993). Nutrition intervention trials in Linxian, China: supplementation with specific vitamin/mineral combinations, cancer incidence, and disease-specific mortality in the general population. J. Natl. Cancer Inst. *85*, 1483–1491.

Bouillet, P., and Strasser, A. (2002). BH3-only proteins- evolutionarily conserved proapoptotic Bcl-2 family members essential for initiating programmed cell death. J. Cell Sci. *115*, 1567–1574.

Bridge, A.J., Pebernard, S., Ducraux, A., Nicoulaz, A.L., and Iggo, R. (2003). Induction of an interferon response by RNAi vectors in mammalian cells. Nat. Genet. *34*, 263–264.

Chance, B., Sies, H., and Boveris, A. (1979). Hydroperoxide metabolism in mammalian organs. Physiol. Rev. *59*, 527–605.

Chiarugi, P. (2008). From anchorage dependent proliferation to survival: lessons from redox signalling. IUBMB Life *60*, 301–307.

Chiarugi, P., and Fiaschi, T. (2007). Redox signalling in anchorage-dependent cell growth. Cell. Signal. *19*, 672–682.

Chong, H.C., Tan, M.J., Philippe, V., Tan, S.H., Tan, C.K., Ku, C.W., Goh, Y.Y., Wahli, W., Michalik, L., and Tan, N.S. (2009). Regulation of epithelial-mesenchymal IL-1 signaling by PPARβ/δ is essential for skin homeostasis and wound healing. J. Cell Biol. *184*, 817–831.

Clément, M.V., and Pervaiz, S. (2001). Intracellular superoxide and hydrogen peroxide concentrations: a critical balance that determines survival or death. Redox Rep. *6*, 211–214.

Desai, U., Lee, E.C., Chung, K., Gao, C., Gay, J., Key, B., Hansen, G., Machajewski, D., Platt, K.A., Sands, A.T., et al. (2007). Lipid-lowering effects of anti-angiopoietin-like 4 antibody recapitulate the lipid phenotype found in angiopoietin-like 4 knockout mice. Proc. Natl. Acad. Sci. USA *104*, 11766–11771.

Desgrosellier, J.S., and Cheresh, D.A. (2010). Integrins in cancer: biological implications and therapeutic opportunities. Nat. Rev. Cancer *10*, 9–22.

Ferraro, D., Corso, S., Fasano, E., Panieri, E., Santangelo, R., Borrello, S., Giordano, S., Pani, G., and Galeotti, T. (2006). Pro-metastatic signaling by c-Met through RAC-1 and reactive oxygen species (ROS). Oncogene *25*, 3689–3698.

Fidler, I.J. (1999). Critical determinants of cancer metastasis: rationale for therapy. Cancer Chemother. Pharmacol. Suppl. *43*, S3–S10.

Galaup, A., Cazes, A., Le Jan, S., Philippe, J., Connault, E., Le Coz, E., Mekid, H., Mir, L.M., Opolon, P., Corvol, P., et al. (2006). Angiopoietin-like 4 prevents metastasis through inhibition of vascular permeability and tumor cell motility and invasiveness. Proc. Natl. Acad. Sci. USA *103*, 18721–18726.

Ge, H., Yang, G., Huang, L., Motola, D.L., Pourbahrami, T., and Li, C. (2004). Oligomerization and regulated proteolytic processing of angiopoietin-like 4. J. Biol. Chem. *279*, 2038–2045.

Giannoni, E., Buricchi, F., Grimaldi, G., Parri, M., Cialdai, F., Taddei, M.L., Raugei, G., Ramponi, G., and Chiarugi, P. (2008). Redox regulation of anoikis: reactive oxygen species as essential mediators of cell survival. Cell Death Differ. *15*, 867–878.

Giannoni, E., Fiaschi, T., Ramponi, G., and Chiarugi, P. (2009). Redox regulation of anoikis resistance of metastatic prostate cancer cells: key role for Src and EGFR-mediated pro-survival signals. Oncogene *28*, 2074–2086.

Hanahan, D., and Weinberg, R.A. (2000). The hallmarks of cancer. Cell *100*, 57–70.

Hennekens, C.H., Buring, J.E., Manson, J.E., Stampfer, M., Rosner, B., Cook, N.R., Belanger, C., LaMotte, F., Gaziano, J.M., Ridker, P.M., et al. (1996). Lack of effect of long-term supplementation with beta carotene on the incidence of malignant neoplasms and cardiovascular disease. N. Engl. J. Med. *334*, 1145–1149.

Irani, K., Xia, Y., Zweier, J.L., Sollott, S.J., Der, C.J., Fearon, E.R., Sundaresan, M., Finkel, T., and Goldschmidt-Clermont, P.J. (1997). Mitogenic signaling mediated by oxidants in Ras-transformed fibroblasts. Science *275*, 1649–1652.

Ito, Y., Oike, Y., Yasunaga, K., Hamada, K., Miyata, K., Matsumoto, S.I., Sugano, S., Tanihara, H., Masuho, Y., and Suda, T. (2003). Inhibition of angiogenesis and vascular leakiness by angiopoietin-related protein 4. Cancer Res. *63*, 6651–6657.

Joneson, T., and Bar-Sagi, D. (1998). A Rac1 effector site controlling mitogenesis through superoxide production. J. Biol. Chem. *273*, 17991–17994.

Kersten, S., Mandard, S., Tan, N.S., Escher, P., Metzger, D., Chambon, P., Gonzalez, F.J., Desvergne, B., and Wahli, W. (2000). Characterization of the fasting-induced adipose factor FIAF, a novel peroxisome proliferator-activated receptor target gene. J. Biol. Chem. *275*, 28488–28493.

Komatsu, D., Kato, M., Nakayama, J., Miyagawa, S., and Kamata, T. (2008). NADPH oxidase 1 plays a critical mediating role in oncogenic Ras-induced vascular endothelial growth factor expression. Oncogene *27*, 4724–4732.

Koster, A., Chao, Y., Mosior, M., Ford, A., Gonzalez-DeWhitt, P., Hale, J., Li, D., Qiu, Y., Fraser, C., and Yang, D. (2005). Transgenic angiopoietin-like (angptl)4 overexpression and targeted disruption of angptl4 and angptl regulation of triglyceride metabolism. Endocrinology *146*, 4943–4950.

Le Jan, S., Amy, C., Cazes, A., Monnot, C., Lamandé, N., Favier, J., Philippe, J., Sibony, M., Gasc, J.M., Corvol, P., et al. (2003). Angiopoietin-like 4 is a proangiogenic factor produced during ischemia and in conventional renal cell carcinoma. Am. J. Pathol. *162*, 1521–1528.

Lee, I.M., Cook, N.R., and Manson, J.E. (1999). Beta-carotene supplementation and incidence of cancer and cardiovascular disease: Women's Health Study. J. Natl. Cancer Inst. *91*, 2102–2106.

Liou, G.Y., and Storz, P. (2010). Reactive oxygen species in cancer. Free Radic. Res. *44*, 479–496.

Minn, A.J., Gupta, G.P., Siegel, P.M., Bos, P.D., Shu, W., Giri, D.D., Viale, A., Olshen, A.B., Gerald, W.L., and Massagué, J. (2005). Genes that mediate breast cancer metastasis to lung. Nature *436*, 518–524.

Mueller, M.M., Peter, W., Mappes, M., Huelsen, A., Steinbauer, H., Boukamp, P., Vaccariello, M., Garlick, J., and Fusenig, N.E. (2001). Tumor progression of skin carcinoma cells in vivo promoted by clonal selection, mutagenesis, and autocrine growth regulation by granulocyte colony-stimulating factor and granulocyte-macrophage colony-stimulating factor. Am. J. Pathol. *159*, 1567–1579.

Murphy, G.J., and Holder, J.C. (2000). PPARγ agonists: therapeutic role in diabetes, inflammation and cancer. Trends Pharmacol. Sci. *21*, 469–474.

Münzel, T., Afanas'ev, I.B., Kleschyov, A.L., and Harrison, D.G. (2002). Detection of superoxide in vascular tissue. Arterioscler. Thromb. Vasc. Biol. *22*, 1761–1768.

Oberley, L.W. (2001). Anticancer therapy by overexpression of superoxide dismutase. Antioxid. Redox Signal. *3*, 461–472.

Oike, Y., Akao, M., Kubota, Y., and Suda, T. (2005). Angiopoietin-like proteins: potential new targets for metabolic syndrome therapy. Trends Mol. Med. *11*, 473–479.

Omenn, G.S., Goodman, G., Thomquist, M., Grizzle, J., Rosenstock, L., Barnhart, S., Balmes, J., Cherniack, M.G., Cullen, M.R., Glass, A., et al. (1994). The beta-carotene and retinol efficacy trial (CARET) for chemoprevention of lung cancer in high risk populations: smokers and asbestos-exposed workers. Cancer Res. *54*, 2038s–2043s.

Padua, D., Zhang, X.H.F., Wang, Q., Nadal, C., Gerald, W.L., Gomis, R.R., and Massagué, J. (2008). TGFβ primes breast tumors for lung metastasis seeding through angiopoietin-like 4. Cell *133*, 66–77.

Paffenholz, R., Bergstrom, R.A., Pasutto, F., Wabnitz, P., Munroe, R.J., Jagla, W., Heinzmann, U., Marquardt, A., Bareiss, A., Laufs, J., et al. (2004). Vestibular defects in head-tilt mice result from mutations in Nox3, encoding an NADPH oxidase. Genes Dev. *18*, 486–491.

Pani, G., Giannoni, E., Galeotti, T., and Chiarugi, P. (2009). Redox-based escape mechanism from death: the cancer lesson. Antioxid. Redox Signal. *11*, 2791–2806.

Pervaiz, S., and Clément, M.V. (2007). Superoxide anion: oncogenic reactive oxygen species? Int. J. Biochem. Cell Biol. *39*, 1297–1304.

Peters, J.M., and Gonzalez, F.J. (2009). Sorting out the functional role(s) of PPARβ/δ in cell proliferation and cancer. Biochim. Biophys. Acta *1796*, 230–241.

Salmon, S.E. (1984). Human tumor colony assay and chemosensitivity testing. Cancer Treat. Rep. *68*, 117–125.

She, Q.B., Solit, D.B., Ye, Q., O'Reilly, K.E., Lobo, J., and Rosen, N. (2005). The BAD protein integrates survival signaling by EGFR/MAPK and PI3K/Akt kinase pathways in PTEN-deficient tumor cells. Cancer Cell *8*, 287–297.

Singh, S., Sadanandam, A., and Singh, R.K. (2007). Chemokines in tumor angiogenesis and metastasis. Cancer Metastasis Rev. *26*, 453–467.

Suh, Y.A., Arnold, R.S., Lassegue, B., Shi, J., Xu, X., Sorescu, D., Chung, A.B., Griendling, K.K., and Lambeth, J.D. (1999). Cell transformation by the superoxide-generating oxidase Mox1. Nature *401*, 79–82.

Sun, Y., and Lodish, H.F. (2010). Adiponectin deficiency promotes tumor growth in mice by reducing macrophage infiltration. PLoS ONE *5*, e11987.

Tan, S.H., Pal, M., Tan, M.J., Wong, M.H.L., Tam, F.U., Teo, J.W.T., Chong, H.C., Tan, C.K., Goh, Y.Y., Tang, M.B.Y., et al. (2009). Regulation of cell proliferation and migration by TAK1 via transcriptional control of von Hippel-Lindau tumor suppressor. J. Biol. Chem. *284*, 18047–18058.

Ushio-Fukai, M., and Nakamura, Y. (2008). Reactive oxygen species and angiogenesis: NADPH oxidase as target for cancer therapy. Cancer Lett. *266*, 37–52.

Wagner, B.A., Evig, C.B., Reszka, K.J., Buettner, G.R., and Burns, C.P. (2005). Doxorubicin increases intracellular hydrogen peroxide in PC3 prostate cancer cells. Arch. Biochem. Biophys. *440*, 181–190.

Wang, Y., Lam, K.S.L., Lam, J.B.B., Lam, M.C., Leung, P.T.Y., Zhou, M., and Xu, A. (2007). Overexpression of angiopoietin-like 4 alters mitochondria

activities and modulates methionine metabolic cycle in the liver tissues of db/db diabetic mice. Mol. Endocrinol. *21*, 972–986.

Wang, Z., Han, B., Zhang, Z., Pan, J., and Xia, H. (2010). Expression of angiopoietin-like 4 and tenascin C but not cathepsin C mRNA predicts prognosis of oral tongue squamous cell carcinoma. Biomarkers *15*, 39–46.

Westhoff, M.A., and Fulda, S. (2009). Adhesion-mediated apoptosis resistance in cancer. Drug Resist. Updat. *12*, 127–136.

Wu, W.S. (2006). The signaling mechanism of ROS in tumor progression. Cancer Metastasis Rev. *25*, 695–705.

Zhan, M., Zhao, H., and Han, Z.C. (2004). Signalling mechanisms of anoikis. Histol. Histopathol. *19*, 973–983.